


AUS Repository

Factors affecting sedimentational separation of bacteria from blood

Item Type	Peer-Reviewed;Article;Postprint
Authors	Pitt, William G.;Alizadeh, Mahsa;Blanco, Rae;Hunter, Alex K.;Bledsoe, Colin G.;McClellan, Daniel S.;Wood, Madison E.;Wood, Ryan L.;Ravsten, Tanner V.;Hickey, Caroline L.;Beard, William Cameron;Stepan, Jacob R.;Carter, Alexandra;Husseini, Ghaleb;Robison, Richard A.;Welling, Evelyn;Torgesen, Rebekah N.;Anderson, Clifton M.
Citation	Pitt, WG, Alizadeh, M, Blanco, R, et al. Factors affecting sedimentational separation of bacteria from blood. Biotechnol Progress. 2020; 36:e2892. https://doi.org/10.1002/btpr.2892
DOI	10.1002/btpr.2892
Publisher	American Institute of Chemical Engineers (AIChE)
Download date	2026-04-22 03:08:49
Link to Item	http://hdl.handle.net/11073/21322

Factors affecting sedimentational separation of bacteria from blood

William G. Pitt¹  | Mahsa Alizadeh¹ | Rae Blanco¹ | Alex K. Hunter¹ |
Colin G. Bledsoe¹ | Daniel S. McClellan¹ | Madison E. Wood² | Ryan L. Wood¹ |
Tanner V. Ravsten¹ | Caroline L. Hickey¹ | William Cameron Beard³ |
Jacob R. Stepan³ | Alexandra Carter¹ | Ghaleb A. Hussein⁴ | Richard A. Robison² |
Evelyn Welling¹ | Rebekah N. Torgesen¹ | Clifton M. Anderson¹

KEYWORDS

bacterial bloodstream infection, bacterial separation, centrifugation, disk design, E. coli, human blood, sedimentation

Abstract

Rapid diagnosis of blood infections requires fast and efficient separation of bacteria from blood. We have developed spinning hollow disks that separate bacteria from blood cells via the differences in sedimentation velocities of these particles. Factors affecting separation included the spinning speed and duration, and disk size. These factors were varied in dozens of experiments for which the volume of separated plasma, and the concentration of bacteria and red blood cells (RBCs) in separated plasma were measured. Data were correlated by a parameter of characteristic sedimentation length, which is the distance that an idealized RBC would travel during the entire spin. Results show that characteristic sedimentation length of 20 to 25 mm produces an optimal separation and collection of bacteria in plasma. This corresponds to spinning a 12-cm-diameter disk at 3,000 rpm for 13 s. Following the spin, a careful deceleration preserves the separation of cells from plasma and provides a bacterial recovery of about $61 \pm 5\%$.

INTRODUCTION

There is increasing need to rapidly identify the species and antibiotic resistance profile of bacteria causing bloodstream infections (BSI) so proper treatment commences quickly. Empirical applications of broad spectrum antibiotics often work satisfactorily, but the general use of these agents may promote the development of resistant bacterial strains.^{1,2} Unfortunately, when undiagnosed BSIs of carbapenem resistant organisms produce a state of sepsis in a patient, the survival rate decreases by 7.6% per hour of ineffective treatment,³ eventually producing a 50% mortality rate.^{4,5} Thus rapid identification of species and antibiotic resistance are essential.

Because the bacterial concentration in BSIs is extremely low (often between 1 and 100 CFU/ml^{6,7}), growth amplification is required for most diagnostics.⁸ While PCR and other genomic amplification techniques are rapid and work well for the high concentrations found in urine,⁹⁻¹¹ they are often ineffective in blood samples due to interfering agents and degradative enzymes.¹²

Our proposed diagnostic process described herein requires only 7 ml of blood, a typical volume collected in vacutainer tubes. The challenge is to rapidly separate a maximal amount of bacteria from $\sim 5 \times 10^9$ red blood cells (RBCs), $\sim 5 \times 10^6$ white blood cells (WBCs) and $\sim 3 \times 10^8$ platelets per ml of blood. Table 1 and Table S1 (Supporting Information) tabulate some important characteristics of blood components.

Component	Density range (g/cm ³)	Density for calculation (g/cm ³)	Shape and size	Sedimentation coefficient ^a	Relative sedimentation coefficient ^b
Red blood cell (RBC) ¹³	1.086–1.122	1.098	Discoidal 2 × 8.1 μm	2.1 × 10 ⁻⁷ s	24
White blood cell (WBC)	1.065–1.092	1.092	Sphere 16 μm diameter	2.3 × 10 ⁻⁷ s	27
Platelet	1.052–1.077	1.075	Sphere 3 μm diameter	2.5 × 10 ⁻⁸ s	3
<i>E. coli</i> ¹⁴	1.08–1.10	1.091	Rod 3.8 × 0.95 μm	8.6 × 10 ⁻⁹ s	1

^a Calculated for single particles using values in Table 1 and PBS-diluted plasma density 1.018 g/cm and viscosity 1.12 mPa s. RBC was modeled as an oblate ellipsoid with diameters of 2.0 and 8.1 μm sedimenting at 3,000 rpm, equivalent radius of 5.85 μm.^{13,15} WBCs and platelets were modeled as nondeformable spheres with diameters given above.¹⁶ *E. coli* was modeled as a 3.8 × 0.95 μm prolate ellipsoid.¹⁴

1 BACKGROUND OF SEPARATION BY SEDIMENTATION

Successful techniques for bacterial separation from blood include microfluidics¹⁷⁻¹⁹ and capture on magnetic beads.²⁰⁻²³ These techniques have been reviewed recently²⁴ and are summarized in Table S2. Although these have high bacterial capture, most are inadequate for clinical use because of low flow rates coupled with the clinical requirements of large blood volumes due to very low bacterial concentrations.

Our novel technique that can handle larger volumes uses centrifugal forces in a rapid and transient mode, which separates particles by both size and density, and not solely density (as is done in conventional centrifugal separation). This is done in a disk-shaped shallow bowl with a partial lid, which is called a hollow disk. This open disk is spun on a motor very rapidly, spinning any fluid contents into a nearly vertical layer on the outer wall. In typical experiments, 7.0 ml of blood and 1.5 ml of buffer are placed in the bowl, and then rapid spinning forms a circumferential pool of diluted blood, about 370 mm in circumference, 2.5 mm deep, and 9 mm tall. The blood cells sediment to the back wall much faster than the bacteria, leaving the bacteria in the plasma. Then upon carefully slowing to a stop, the blood cells at the back wall slump down into a capture chamber, and the plasma (containing the bacteria) flows into a collection area (see Figure 1).

We previously published studies using only one size of a hollow disk that separated bacteria from ml quantities of blood in ~5 min.^{25,26} In this present study, we varied the size of the disk, rotational speed and spinning time. Herein we report our hollow disk spinning parameters that maximize bacterial recovery while minimizing RBC contamination, using 7 ml of human blood and producing an optimum bacterial recovery of about 61% in only 2 min.

1.1 | Sedimentation velocity and length

Sedimentation of small isolated particles in a viscous fluid occurs because acceleration, buoyant and drag forces combine to produce a steady-state sedimentation velocity of the particle in the fluid. In a rotating system, the sedimentation velocity is given by (see Supporting Information for the derivation):

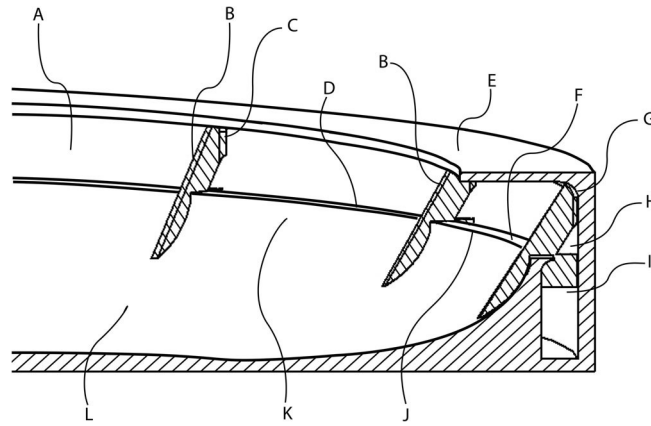


FIGURE 1 Cutaway section of a typical hollow disk design.

(a) Upper chamber of vestibule. (b) Baffle. (c) Fillet of baffle. (d) Back edge of weir. (e) Lid. (f) Top of weir. (g) Fillet on lid. (h) Window in baffle. (i) Trough of vestibule. (j) Inward edge of weir. (k) Slope. (l) Bowl

$$v_s = \frac{D_p^2(\rho_p - \rho_f)\sqrt{R^2\omega^4 + g^2}}{18\mu K} \quad (1)$$

In this equation, D_p is the particle diameter, ρ is the density of particle or fluid, R is the radial position of the particle, ω is the angular velocity, g is the gravitational constant, and μ is the fluid viscosity. The sedimentation velocity reaches a steady-state value in less than a ms (see Supporting Information). K is a correction factor that arises when the particle concentration increases to the point that the particles no longer follow Stokes law.^{27,28} Thus for a dilute solution of small hard spheres $K = 1$. However, in blood $K \neq 1$ because of the very high concentration of flexible blood cells and platelets. Estimates of K as a function of concentration have been made for randomly arranged hard spheres²⁷ or spheres of differing sizes.²⁹

The sedimentation coefficient, s , is defined as the ratio of the sedimentation velocity to the driving acceleration, whether it be gravity (g) or centrifugal acceleration ($R\omega^2$)³⁰:

$$s = \frac{dR/dt}{\omega^2 R} = \frac{m}{f} \left(1 - \frac{\rho_p}{\rho_f} \right), \quad (2)$$

where R is the radial position of the particle, m is the mass of the particle, f is the drag force on the particle. For a short particle displacement in our thin-layer centrifugal system in a hollow disk, dR/dt is the sedimentation velocity, v_s . Table 1 gives estimates of sedimentation coefficients for various blood components (assuming $K = 1$) and presents some of their key physical parameters.

Our overall research objective is to quickly and efficiently separate blood cells out of plasma while retaining bacteria; this paper describes our efforts to study this separation as a function of process speed and time. Because the movement of RBCs and bacteria is the time integral of sedimentation velocity given by Equation (1), a parameter was formulated by which all experiments of differing disk size, spinning speed, and duration, can be correlated. This parameter is the time integral of the velocity (producing a characteristic length scale) that a single ($K = 1$) 8- μm -diameter spherical particle would move, according to Equation (1). This idealized particle has the density of a RBC (1.098 g/ml) and sediments through plasma having a density of 1.024 g/ml and a viscosity of 1.95 mPa s at 20°C.³¹ This characteristic length, \mathcal{L}_s , hereafter named sedimentation length, is given by

$$\mathcal{L}_s(R, \omega, t) = \int_0^t v_s(R, \omega, t) dt. \quad (3)$$

This time integral includes the time during acceleration and deceleration of the disk. Thus \mathcal{L}_s incorporates all forces on the blood components during the entirety of any type of spin. We hypothesize that experiments employing differing diameters, speeds and durations, yet having identical values of \mathcal{L}_s , will have identical physical distributions of cells and bacteria within the fluid in the disk. Our results support this hypothesis and provide parameters from which bacterial separation processes can be designed for other disk sizes and speeds, based on bacterial separation as a function of \mathcal{L}_s . This enables future design of spinning disk systems for clinical applications.

2 | MATERIALS AND METHODS

2.1 | Description of disk features

Figure 1 illustrates the 12-cm-diameter disk used in this study, which is the same disk used in previous studies with very low bacterial load.²⁵ For disks of different size (10- and 16-cm-diameter) the basic design features (number of baffles, trough volume, vestibule chamber volume) were scaled linearly with disk diameter (see Table 2). Key design features are (a) weir which holds back the cell-pack as spinning stops and the cell-pack slumps into the trough; (b) slope which is nearly vertical where it meets the inward edge of the top of the weir; (c) vestibule which is the space occupied by blood during spinning and is divided into the trough and the upper chamber; (d) baffles which

TABLE 2 Hollow disks

Disk diameter (cm)	Number of baffles	Trough volume (ml)	Vestibule volume (ml)	Blood (ml)	PBS added (ml)
10	13	3.22	7.08	5.83	1.25
12	16	3.97	8.50	7.00	1.5
16	21	5.33	11.33	9.33	2.0

promote drainage of plasma and which have windows in the upper chamber and trough; and (e) lid and back wall which form the top and back boundaries of the vestibule. We placed “windows” in the baffles to allow lateral flow of blood, cell-pack and plasma in the vestibule during spin-up and plasma drainage. The baffles did not extend to the bottom of the trough to facilitate cleaning the cell-pack from the trough between experiments.

Some design features were updated since our previous publication.²⁶ For example, a ring of rapid-prototyping polymer material was printed along the lower outside edge of the disk in order to lower the center of gravity of the disk, thus increasing the stability during spinning.

Disks were printed with an Objet30 Prime System (Stratasys, Eden Prairie, MN) using VeroClear™ resin as described previously.²⁶ The programmable and precision control of spinning was done using LabView software and a Maxon motor (model 301039) as described previously.³²

2.2 | Blood, bacteria, and spinning

Human blood was obtained from volunteers by venipuncture and collected into EDTA-containing vacutainers (BD #366643, Becton Dickinson) under an IRB-approved protocol at Brigham Young University. Bacteria used for all the experiments were *Escherichia coli* (strain BL21), streaked from frozen stock and grown overnight with shaking in nutrient broth. Bacteria were washed in PBS before dilution and inoculation into blood at a concentration of around 10^6 CFU/ml in these experiments.²⁶ The Supporting Information presents more detail. Depending on disk diameter (Table 2), 1.25, 1.5, or 2 ml of PBS was pipetted into a ring in the bowl of the disk and 5.83, 7.00, or 9.33 ml, respectively, of bacteria-spiked blood were pipetted into the ring of PBS just before spinning.

When spinning started, blood was quickly thrown into the vestibule and sedimentation began. The ramp-up acceleration was 500 rpm/s. The hold velocity varied from 1,000 to 4,000 rpm and the hold time was 0 to 120 s depending on experimental parameters.

Finally the disk was carefully slowed, following a deceleration velocity profile that was determined through experimentation to avoid mixing of the clear plasma and the cell-pack.³² If deceleration was too fast, the plasma and blood cells remixed, and the plasma was no longer transparent amber color. Even upon slow careful deceleration, sometimes there was a small streak of red cells in the transparent plasma. After spinning, the degree of remixing of plasma and cell-pack layers, and the amount of steaking of RBCs, was visually assessed.

The plasma was collected by pipette, weighed, and the volume calculated assuming plasma density of 1.024 g/ml.

2.3 | Quantitation of plasma, bacteria, RBC

As published previously, serial dilution and plating were used to estimate the number of bacteria in spiked whole blood and in recovered plasma.²⁶ RBC concentration was estimated by spectroscopic methods.

To facilitate comparison of experiments with various disk sizes, the efficiency of plasma recovery is defined as:

$$\epsilon_{pl} = \frac{V_{pl} - V_{PBS}}{V_{blood}}, \quad (4)$$

where V_{pl} , V_{blood} , and V_{PBS} are the volumes, respectively, of recovered plasma, original blood pipetted into the disk, and PBS added to the blood. This parameter represents the volume fraction of blood placed on the disk that eventually flowed over the weir and was collected. If adding PBS to blood, changing disk size, or modifying weir design increases ϵ_{pl} , then greater total recovery of bacteria is expected. The value $1 - \epsilon_{pl}$ represents the volume fraction of blood left in the disk.

The “concentration recovery” of bacteria is the ratio of the bacterial concentration in recovered plasma, $C_{B,pl}$, and the concentration in undiluted blood, $C_{B,bl}$:

$$C_B^* = \frac{C_{B,pl}}{C_{B,bl}}. \quad (5)$$

When blood is diluted with PBS, C_B^* is expected to be less than unity even if no enrichment or depletion of bacteria in the plasma phase occurs. From that initial diluted value, C_B^* is expected to increase for a short time as bacteria sediment out of the blood cell-pack into plasma, and then decrease with more spinning time as bacteria sediment into the cell-pack and are therefore not recovered in the plasma.

The efficiency of bacterial recovery is the ratio of all bacteria recovered via pipetting to all bacteria placed in the disk:

$$\epsilon_{BR} = \frac{V_{pl} - C_{B,pl}}{V_{blood} C_{B,bl}}, \quad (6)$$

To quantitate minimization of RBC in the recovered plasma, the normalized RBC recovery is defined as the ratio of RBCs in the recovered plasma ($C_{RBC,pl}$) to the RBC concentration in undiluted blood

($C_{RBC,bl}$):

$$C_{RBC}^* = \frac{C_{RBC,pl}}{C_{RBC,bl}}. \quad (7)$$

In these experiments, this number is always less than unity since the blood was diluted with PBS prior to spinning.

Red cell packing in the trough was estimated by carefully pipetting red cell-pack material from the trough following spinning at 3,000 rpm for 48 s. The hematocrit of this material was measured by placing it in a capillary tube and spinning at 1,300g for 10 min.³³

3 | RESULTS

In experiments described herein, we correlated the disk size and disk operation with three key parameters that affect the quality of bacterial recovery and that will affect subsequent processing (genetic or phenotypic analysis) of bacteria found in blood: (a) volume of recovered plasma; (b) bacterial concentration in recovered plasma; and (c) concentration of blood cells in recovered plasma. Our goal is to maximize the first two of these parameters while minimizing the third. However, the concentration of bacteria and blood cells in recovered plasma are highly correlated, and one cannot maximize bacteria recovery while minimizing RBC contamination in recovered plasma.

We first report experimental parameters affecting the volume of recovered plasma. Then we present parameters affecting the concentrations of bacteria and blood cells in the plasma. For those parameters that relate to the sedimentation velocity, the data will be presented as a function of L_s , which correlates the distance traveled by cells.

3.1 | Plasma quality and volume

Clarity of plasma refers to the qualitative assessment of RBCs visually observed in plasma. Deviation from clear amber-colored plasma comes in two forms: remixing and streaking. Remixing refers to turbulent mixing of separated plasma and cell-pack that sometimes occurred near completion of disk deceleration. If the disk were decelerated too quickly, the clear plasma would mix with the adjacent cellpack layer, displaying a uniform orange hue, from yellow-orange to red, depending upon how much remixing occurred. Remixing is a manifestation of Kelvin–Helmholtz instability and is reported elsewhere.³²

Streaking refers to the observation that often plasma flowing down had streaks of RBCs in the otherwise clear (amber) plasma, and is clearly distinguishable from mixing (Figure S1). Streaking is undesirable because it introduces cells back into the clarified plasma. We noted that streaking increased when using blood of higher hematocrit and when plasma drained from a single point along the edge of the weir. The amount of RBCs returned back into the plasma by streaking was measured by the RBC-recovery parameter, C_{RBC}^* (Equation 7).

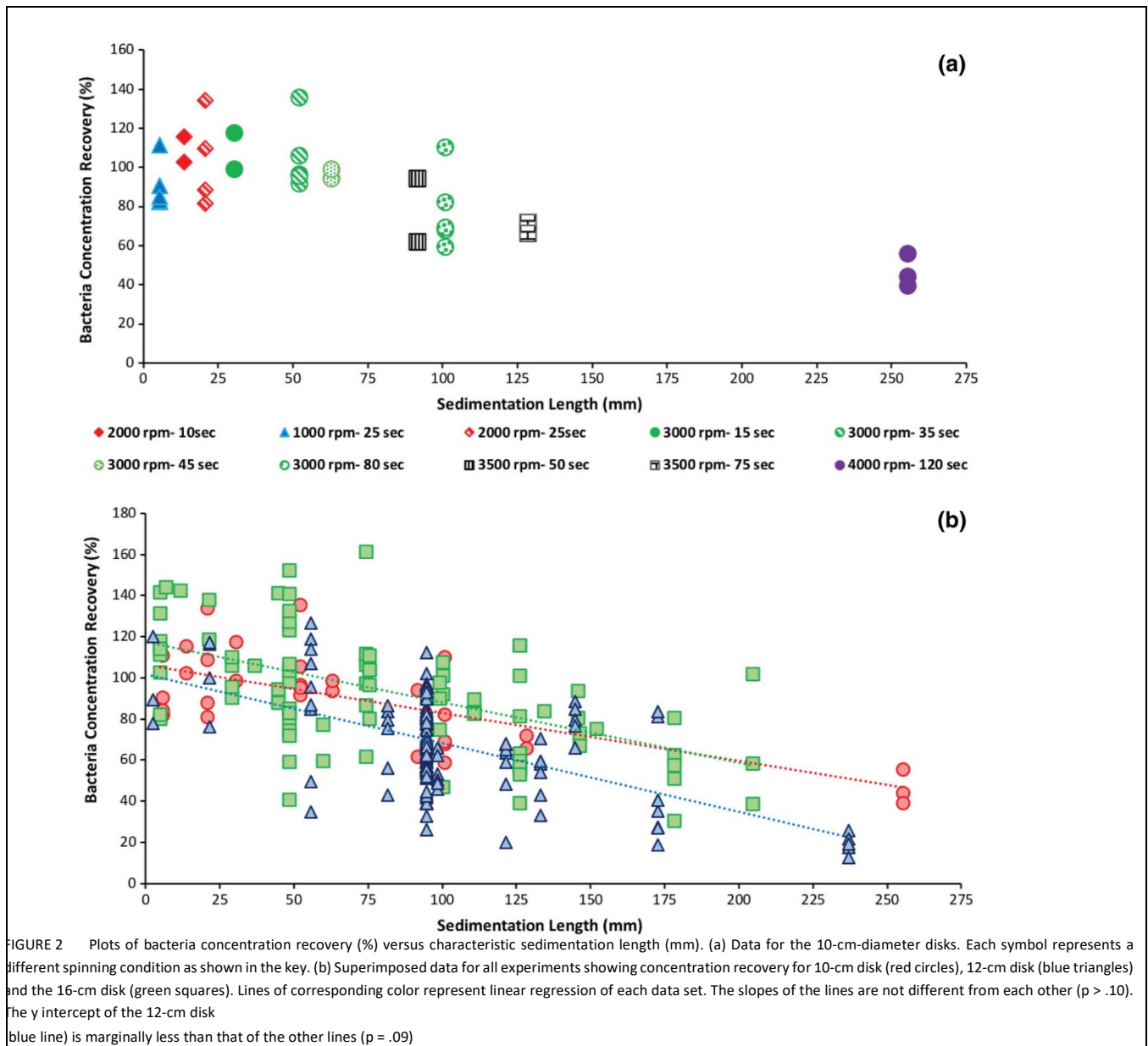
Plasma volume. While the recovered plasma volume is larger for larger disks, it does not appear to be a strong function of L_s for a single disk size (Figure S2A). We note that in general, the largest volumes recovered were those from experiments with very small L_s (<10 mm), such as when blood was spun up to 1,000 or 2,000 rpm, and then immediately decelerated. We postulate that under these spinning conditions, the front slope, having been wetted with blood during spinup, had not dried completely, and was more wettable toward plasma drainage. To determine if disk size has any additional influence on plasma recovery, the efficiency of plasma recovery (ϵ_{pi}) was calculated (Equation 4 and Figure S2B). Statistical analysis of ϵ_{pi} indicates that 12- and 16-cm disks do not have different recoveries from each other, but both have better plasma recovery efficiency than the 10-cm diameter disk ($p < .05$).

3.2 | Concentration recovery

Figure 2 and Figure S3 show plots of bacterial concentration recovery as a function of L_s for three disk sizes. They all follow the postulated trend that concentration recovery should decrease as L_s increases. Various experiments involving different disk sizes, rotational velocities and spin durations all generally map to a common trend line. Figure 2b shows the superposition of data from the three disk sizes. When the slopes of linear regression of each data set from each disk size were analyzed, there is no statistically significant difference between the slopes ($p > .10$). However, the y-axis intercepts of the 12-cm disk line is marginally less than that of the 10-cm and 16-cm disk intercepts ($p = .09$).

Extrapolation of these lines to the x-axis indicates that at L_s values from 300 to 400 mm, the bacterial recovery would be negligible. Concentration recoveries of bacteria at small L_s are much greater than 82%, a value that would be expected (7.0 ml of blood diluted with 1.5 ml of PBS) in the absence of sedimentation of bacteria into or out of the plasma phase. We hypothesize that this “higher-than expected” increase in bacterial concentration occurs because bacteria are excluded from the volume occupied by blood cells, and as blood cells quickly sediment to the back wall, the volume flux of red cells displaces plasma in the opposite direction toward the axis of rotation. Apparently, this “backflow” of plasma may carry some bacteria with it, despite the proximity of blood cells that could trap bacteria within the region of sedimenting and concentrating RBCs. Not all bacteria escaped this condensing cell-pack, but some may escape to increase the bacterial concentration in the plasma at short times. These data suggest that there must be a maximum in concentration recovery somewhere between sedimentation lengths of zero and 50 mm.

3.3 | Total bacterial recovery



Total bacterial recovery was calculated for each experiment by Equation (6). Figure 3 shows that these data in general follow the same trend as the concentration recovery (see also Figure S4A). Again at short L_s , these values are much higher than would be expected based on dilution alone. For example, if we use the average recovered plasma volume for the 12-cm disk experiments of 3.7 ml, and divide by the volume in the disk (8.5 ml), we would expect to obtain only 36% of the bacteria in the disk if no concentration enhancement during sedimentation occurred. Values higher than 36% indicate that the bacteria become concentrated in the plasma, most probably because the sedimenting cell-pack expels plasma, which convects some bacteria backward (see Section 5). As spinning progresses, some bacteria sediments toward or into the cell-pack and are not recovered. We postulate that the maximum in total recovery is at some sedimentation length from 25 to 50 mm. The total bacterial recovery in this range ($25 < L_s < 50$) is 60.7% ($\pm 5.0\%$, 95% confidence interval [CI], $n = 28$) when averaged over all experiments.

3.4 | Red cell recovery

As indicated by the sedimentation coefficients of Table 1 derived from Equations (1) and (2), RBCs sediment about 24 times faster than bacteria. Since bacteria appear to be totally sedimented at $L_s = 400$ mm, we would expect RBCs to be sedimented at $1/24$ of that length ($L_s \sim 17$ mm), which is a rough estimate because it does not account for the difference in drag due to differences in the shape, flexibility and concentration of RBCs and of bacteria. Despite this rough estimate, the red cell recovery data shown in Figure 4 (12-cm disk) indicate that RBC recovery decreases from $L_s = 0$ to ~ 20 mm, and then remains fairly constant for sedimentation lengths far above 20 mm.

The nonzero value of RBC recovery, even at large L_s is attributed to experimental observation of streaking, and not from remixing, nor from incomplete separation of plasma from RBCs (with the exception of $L_s < 15$ mm, in which incomplete separation was observed). Because of the small dilution with PBS, if no RBC sedimentation were to occur, we would expect that as L_s approaches 0, $\epsilon_{RBC} = 7.0/8.5 = 0.82$, a value consistent with Figure 4.

We attribute the residual RBCs in the plasma for $L_s < 25$ mm to streaking, and posit that the decrease in ϵ_{RBC} between sedimentation lengths of 0–25 mm is due to sedimentation of blood cells into the vestibule.

Streaking was observed in nearly all experiments with Hct above 35, which suggests that the trough volume is not sufficient to accommodate all the RBCs. Measurements taken from the trough after spinning reveal that RBC packing is only about 85 vol%, and the current trough volume is apparently under-designed for blood of high hematocrit. More plots of RBC recovery are found in Figure S5.

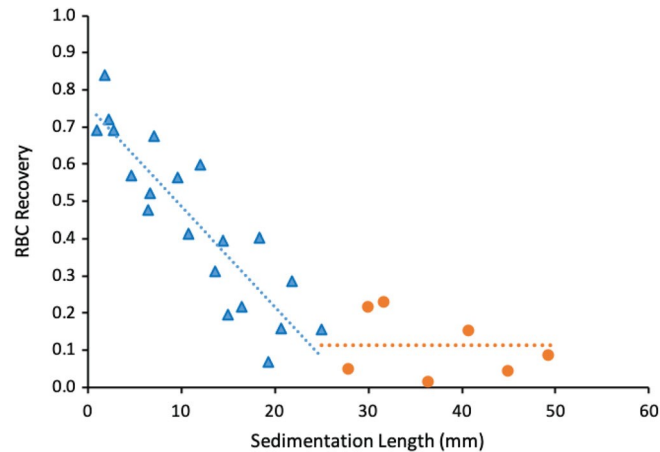


FIGURE 4 Red blood cell recovery versus sedimentation length for the 12-cm-diameter disk. In these experiments the spinning speed was 1,000 rpm to keep the characteristic length small. Blue triangles and blue dotted line represent data for characteristic length < 25 . Yellow circles and yellow dotted line represent data for characteristic length > 25 . The lines are linear regressions within each region.

4 | DISCUSSION

We have developed a fairly simple and rapid method for separating bacteria from human blood cells using a hollow rotating disk. Results show that total bacterial recovery from 7 ml of spiked human blood ranges from ~61 to 0%, depending on the value of L_s . While this recovery is slightly lower than other methods in the literature (Table S2), this can be accomplished in 2 min on a large volume of blood. A maximum of $61 \pm 5\%$ (mean and 95% CI) recovery apparently occurs between L_s values of 20–50 mm. The sedimentation of the vast majority of RBCs appears to be completed at $L_s = 25$ mm, but streaking with blood of higher hematocrit introduces some RBCs back into the plasma.

Suspended particles of similar densities are very difficult to separate from each other by isopycnic centrifugation. If their sizes are only slightly different, separation by filtration becomes challenging—particularly if the smaller-sized particles (bacteria) are in the minority by number, as the high number of larger blood cells will block the filter pores and prevent most of the bacteria from passing through the filter. For diagnostic processes requiring rapid separation with very little process fluid, the transient sedimentation process described herein will separate particles from blood cells of similar density yet slightly different size, even when bacteria are in the vast minority.

The key to this rapid separation is to spread the blood volume over a large surface area within the hollow device, creating a thin layer of blood—much thinner than with conventional plasma separation by centrifugation in a test tube. While similar rotation and sedimentation velocities are achieved both in our hollow disk and in conventional centrifuge tube methods, the 2-mm distance is much shorter in our hollow disk than the ~50 mm distance in a 10-ml centrifuge tube.

A promising observation is that concentration recovery of bacteria in plasma is much greater than calculated solely on the dilution of blood by PBS. This can happen only if bacteria are carried toward the axis of rotation by plasma squeezed out of the cell-pack as the blood cells consolidate at the back wall of the vestibule. The sedimentation velocity in Equation (1) is defined as the velocity of a bacterium relative to the surrounding fluid. Although there is always sedimentation of bacteria in the outward direction relative to the local flow, when bacteria are entrained in plasma that is flowing inwardly more rapidly than the outward sedimentation velocity, the net displacement of bacteria is into the plasma phase, at least until the surrounding blood cells have ceased consolidation in the cell-pack. Apparently, much of the net-inward-moving bacteria avoid being trapped by nearby blood cells moving outwardly and escape into the plasma phase. Adding PBS as a diluent to blood spreads the blood cells further from each other and is postulated to allow more bacteria to escape to the plasma phase, although experiments to verify this have not yet been completed.

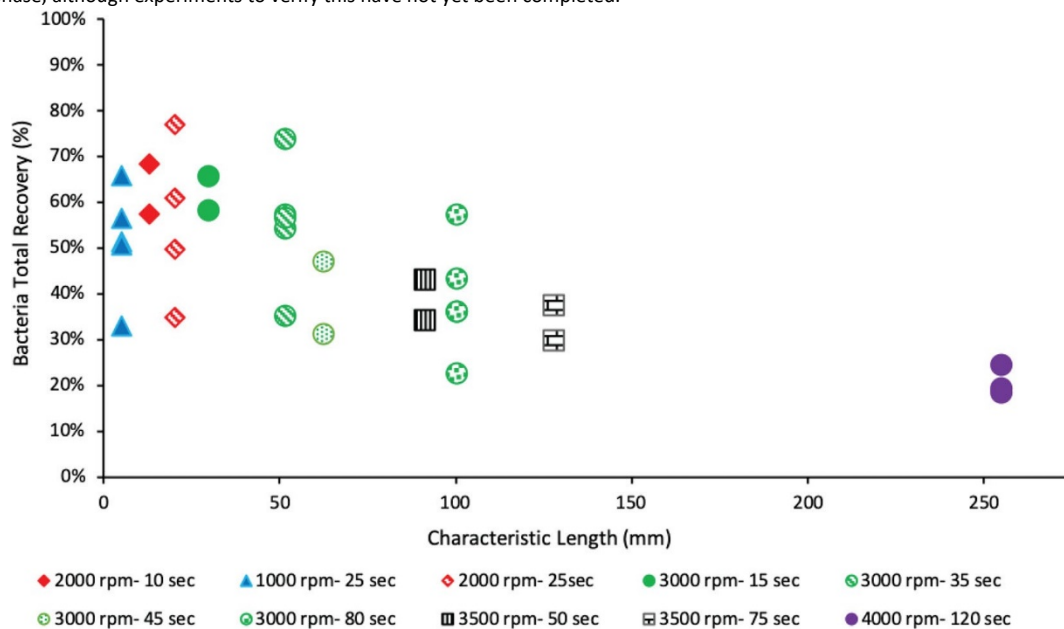


FIGURE 3 Bacteria total recovery versus sedimentation length for the 10-cm-diameter disk. Spinning speed and hold time varied from 1,000 rpm and from 10 to 120 s. Each symbol represents a different spinning condition as shown in the key. Blue symbols are spinning at 1,000 rpm; red symbols are spinning at 2,000 rpm; green symbols are spinning at 3,000 rpm; black symbols are spinning at 3,500 rpm; violet symbols are spinning at 4,000 rpm

This observation that bacterial concentration in the plasma phase increases initially and then decreases at long L_s indicates there is maximum in bacterial concentration sometime during the spin. This maximum should occur around the time that blood cells finish consolidation in the cell-pack. Because of noise in the RBC-recovery data, we cannot easily determine at what L_s the cells are consolidated, but completion of consolidation may occur at L_s values from 20 to 25 mm, which is consistent with the data of bacterial concentration recovery.

An intriguing observation is that the values of L_s for RBC consolidation into a pack in the vestibule is ~ 20 mm, yet the longest distance any RBC had to travel was just over 1.5 mm. Apparently the actual velocities of cells (and bacteria) are much slower than predicted by Stokes law and Equation (1). Several factors combine to reduce the sedimentation velocity.

First, for an isolated sphere in creeping flow, f (the friction factor of Equation 2) is given by Stokes law, in which case Equation (2) reduces to Equation (1). However, for non spherical particles, soft flexible particles, and crowded particles, f deviates from Stokes law, and is modeled by.

$$f = 3\pi\mu\nu_s D_p K_{total} \quad (8)$$

where K_{total} accounts for many corrections and can be modeled as the product of k_{shape} , k_{flex} , and K

$$K_{total} = k_{shape} k_{flex} K \quad (9)$$

where K is the crowdedness correction introduced in Equation (1). D_p is the equivalent spherical diameter of a spheroid. For example, the average RBC volume in a healthy adult is $\sim 94 \mu\text{l}$,¹³ which corresponds to $D_p = 5.64 \mu\text{m}$.

Human RBCs are not spherical, but have a biconcave discoidal shape that is from 7.5 to 8.7 μm in diameter and 1.7 to 2.2 μm in thickness.¹³ When modeling a RBC as a solid oblate spheroid with major diameter 8 μm and minor diameter 2 μm , the k_{shape} is 1.17.³⁰

When RBCs sediment at very high centrifugal forces, they change shape from biconcave to a more streamlined shape³⁴ and experience “tank-treading,” both of which will reduce k_{flex} .^{15,35} At the 3,000 rpm used in this study, shape change would increase their sedimentation velocity 1.9-fold (compared to 0 rpm); thus k_{flex} is 0.52.¹⁵

As particles moving through a fluid approach each other, the disturbance of the hydrodynamic flow fields around the particles interact with each other, leading to more drag force and slowing their movement. Numerical studies of Tenneti et al indicate that drag forces are increased about 10-fold, 20-fold, and 40-fold for suspensions of spheres with volume fractions of 0.3, 0.4, and 0.5, respectively.²⁹ Thus the “ K ” in Equations (1) and (9) would take on values between 10 and 40, depending on the hematocrit of the blood. When blood with hematocrit of 42.5 is partly diluted to a hematocrit of 35 (as in our experiments), K is ~ 15 . Combining all these corrections, K_{total} is estimated to be ~ 9 . Thus, the sedimentation coefficient for flexible RBCs in our experiments is calculated to be $\sim 1.4 \times 10^{-8}$ s. At a distance of 5.85 cm from the center of a hollow disk spinning at 3,000 rpm, we calculate the sedimentation velocity to be 0.082 mm/s, relative to the surrounding fluid (a mixture of plasma and PBS with a density of 1.018 g/ml and viscosity of 1.12 mPa s).

In a closed container like a centrifuge tube or hollow disk, the movement of RBCs toward the wall displaces fluid back against the movement of the cells. Because the sedimentation velocity is relative to the surrounding fluid, the absolute velocity relative to the axis of rotation is greatly reduced by the backflow of fluid proportional to $(1-\phi)$, where ϕ is the volume fraction of sedimenting particles (approximately the hematocrit of the blood suspension). For a physical travel of only 1 mm and accounting for the backflow of plasma, RBCs (at Hct = 35) should be cleared from plasma in 18.8 s. However, the clearance will take longer than this because as the cells start to consolidate and crowd together, the K -value increases exponentially with local hematocrit and eventually exceeds 100; and thus RBC velocity slows drastically as the cell-pack consolidates. Obviously, rigorous modeling is needed to calculate the time and rotational velocity needed to totally consolidate the cell-pack in the vestibule.

There have been measurements of sedimentation velocity of RBCs. For example, Bar et al calculated sedimentation coefficients in diluted blood from centrifugation experiments at various rotational accelerations. These experimental measurements include contributions to faster sedimentation for streamlined shape change at high rpms, and slower sedimentation due to crowding of cells and nonspherical shape. The reported sedimentation coefficients for washed RBC at ϕ of 0.15 in saline (at 1,500 rpm) are from 0.81×10^{-7} to 1.1×10^{-7} s.¹⁵ These reported values apparently are velocities relative to a fixed reference frame (the tube) and not relative to the local fluid velocity.

Of course, the real question regards the sedimentation behavior of bacteria. As bacteria are only slightly smaller than the RBCs and they experience the same volume fraction of surrounding suspended solids, we expect that the “ K ” for bacteria is on the same order as that of RBCs. More precise modeling of both bacteria and RBC transport in the vestibule is ongoing and will be published later.

While this paper points out progress in the disk design and operational parameters to increase recovered plasma volume and decrease residual RBCs, the process is not yet perfect, and further studies and modifications are ongoing.

5 | CONCLUSIONS

The hollow disk is designed to maximize the volume of plasma recovered using various techniques such as making the slope steep so plasma will easily flow by gravity. Various sizes of disks with similar weir and slope design were made to examine the effect of disk size, and of spinning time and speed.

Results show that the bacterial concentration in recovered plasma depends strongly on spinning parameters and disk size. At very short times, bacterial concentration in plasma increases to values greater than in blood, indicating that sedimentation of blood cells toward the back wall forces plasma inward toward the axis of rotation and entrains some bacteria, initially enriching the plasma phase with bacteria. With more spinning time, bacteria sediment toward the back wall of the vestibule and merge into the cell-pack, thus reducing the average concentration in the plasma phase.

The characteristic sedimentation length \mathcal{L}_s is a useful parameter for comparing disks of various designs and sizes, and differing velocity profiles. Dozens of experiments showed strong correlation of bacterial concentration recovery with \mathcal{L}_s . Bacterial concentration has a maximum around $\mathcal{L}_s = 20\text{--}25$ mm, and then decreases to near zero at $\mathcal{L}_s = 400$ mm. Characteristic lengths of 25 mm are quickly accomplished. For example, this can be done on a 12-cm disk with a 6-s spin-up to 3,000 rpm, a 7-s hold at 3,000 rpm, and a slower spin down over 100 s, for total time under 2 min. The spin-down velocity profile must be carefully controlled to prevent mixing of the separated plasma with the blood cell-pack.

Blood cells sediment into a consolidated cell-pack, most probably at around $\mathcal{L}_s = 25$ mm. The consolidation is postulated to produce the maximum in average bacterial concentration at this same \mathcal{L}_s .

ACKNOWLEDGMENT

We gratefully acknowledge funding by National Institutes of Health grant R01AI116989.

CONFLICT OF INTEREST

There are no conflicts of interest of any of the authors and any technologies described herein.

ORCID

William G. Pitt  <https://orcid.org/0000-0002-6043-3452>

REFERENCES

1. Karam G, Chastre J, Wilcox MH, Vincent JL. Antibiotic strategies in the era of multidrug resistance. *Crit Care*. 2016;20(1):136.
2. Ventola CL. The antibiotic resistance crisis: part 1: causes and threats. *Pharm Ther*. 2015;40(4):277-283.
3. Kumar A, Roberts D, Wood KE, et al. Duration of hypotension before initiation of effective antimicrobial therapy is the critical determinant of survival in human septic shock. *Crit Care Med*. 2006;34(6):1589-1596.
4. Vergara-Lopez S, Dominguez MC, Conejo MC, Pascual A, RodriguezBano J. Lessons from an outbreak of metallo-beta-lactamase-producing *Klebsiella oxytoca* in an intensive care unit: the importance of time at risk and combination therapy. *J Hosp Infect*. 2015;89(2):123-131.
5. Zarkotou O, Pournaras S, Tselioti P, et al. Predictors of mortality in patients with bloodstream infections caused by KPC-producing *Klebsiella pneumoniae* and impact of appropriate antimicrobial treatment. *Clin Microbiol Infect*. 2011;17(12):1798-1803.
6. Yagupsky P, Nolte FS. Quantitative aspects of septicemia. *Clin Microbiol Rev*. 1990;3(3):269-279.
7. Kregger BE, Craven DE, Carling PC, McCabe WR. Gram-negative bacteremia. III. Reassessment of etiology, epidemiology and ecology in 612 patients. *Am J Med*. 1980;68(3):332-343.
8. Opota O, Jatou K, Greub G. Microbial diagnosis of bloodstream infection: towards molecular diagnosis directly from blood. *Clin Microbiol Infect*. 2015;21(4):323-331.

9. Mezger A, Gullberg E, Goransson J, et al. A general method for rapid determination of antibiotic susceptibility and species in bacterial infections. *J Clin Microbiol*. 2015;53(2):425-432.
10. Schoepp NG, Khorosheva EM, Schlappi TS, et al. Digital quantification of DNA replication and chromosome segregation enables determination of antimicrobial susceptibility after only 15 minutes of antibiotic exposure. *Angew Chem Int Ed Engl*. 2016;55(33):9557-9561.
11. Schoepp NG, Schlappi TS, Curtis MS, et al. Rapid pathogen-specific phenotypic antibiotic susceptibility testing using digital LAMP quantification in clinical samples. *Sci Transl Med*. 2017;9(410):eaal3693.
12. Hedman J, Radstrom P. Overcoming inhibition in real-time diagnostic PCR. In: Wilkes M, ed. *PCR Detection of Microbial Pathogens*. Vol 943. Totowa, New Jersey: Humana Press; 2013:17-48.
13. Diez-Silva M, Dao M, Han JY, Lim CT, Suresh S. Shape and biomechanical characteristics of human red blood cells in health and disease. *Mrs Bull*. 2010;35(5):382-388.
14. Woldringh CL, Binnerts JS, Mans A. Variation in *Escherichia coli* buoyant density measured in Percoll gradients. *J Bacteriol*. 1981;148(1):58-63.
15. Bar S, Streichman S, Marmur A. The sedimentation coefficient of red blood cell suspensions as a measure of deformability: continuous monitoring of centrifugal sedimentation. *Chem Eng Sci*. 1997;52(6):1059-1064.
16. Recktenwald D, Radbruch A. *Cell Separation Methods and Applications*. New York: Dekker; 1998.
17. Hou HW, Bhattacharyya RP, Hung DT, Han J. Direct detection and drug-resistance profiling of bacteremias using inertial microfluidics. *Lab Chip*. 2015;15(10):2297-2307.
18. Zelenin S, Hansson J, Ardabili S, Ramachandraiah H, Brismar H, Russom A. Microfluidic-based isolation of bacteria from whole blood for sepsis diagnostics. *Biotechnol Lett*. 2015;37(4):825-830.
19. Ohlsson P, Petersson K, Augustsson P, Laurell T. Acoustic impedance matched buffers enable separation of bacteria from blood cells at high cell concentrations. *Sci Rep*. 2018;8(1):9156.
20. Lopes AL, Cardoso J, Dos Santos FR, et al. Development of a magnetic separation method to capture sepsis associated bacteria in blood. *J Microbiol Methods*. 2016;128:96-101.
21. Malic L, Zhang X, Brassard D, et al. Polymer-based microfluidic chip for rapid and efficient immunomagnetic capture and release of *Listeria monocytogenes*. *Lab Chip*. 2015;15(20):3994-4007.
22. Kang JH, Super M, Yung CW, et al. An extracorporeal blood-cleansing device for sepsis therapy. *Nat Med*. 2014;20(10):1211-1216.
23. Lee JJ, Jeong KJ, Hashimoto M, et al. Synthetic ligand-coated magnetic nanoparticles for microfluidic bacterial separation from blood. *Nano Lett*. 2014;14(1):1-5.
24. Pitt WG, Alizadeh M, Husseini GA, et al. Rapid separation of bacteria from blood—review and outlook. *Biotechnol Prog*. 2016;32(4):823-839.
25. Buchanan CM, Wood RL, Hoj TR, et al. Rapid separation of very low concentrations of bacteria from blood. *J Microbiol Methods*. 2017; 139:48-53.
26. Alizadeh M, Wood RL, Buchanan CM, et al. Rapid separation of bacteria from blood—chemical aspects. *Colloids Surf B Biointerfaces*. 2017;154:365-372.
27. Sangani AS, Acrivos A. Slow flow through a periodic array of spheres. *Int J Multiph Flow*. 1982;8(4):343-360.
28. Zick AA, Homsy GM. Stokes-flow through periodic arrays of spheres. *J Fluid Mech*. 1982;115:13-26.
29. Tenneti S, Garg R, Subramaniam S. Drag law for monodisperse gas-solid systems using particle-resolved direct numerical simulation of flow past fixed assemblies of spheres. *Int J Multiph Flow*. 2011;37(9):1072-1092.
30. Hiemenz PC, Rajagopalan R. *Principles of Colloid and Surface Chemistry*. 3rd ed. New York: Marcel Dekker; 1997.
31. Brust M, Schaefer C, Doerr R, et al. Rheology of human blood plasma: viscoelastic versus Newtonian behavior. *Phys Rev Lett*. 2013;110(7):078305.
32. Wood RL, Whitehead JP, Hunter AK, McClellan DS, Pitt WG. An experimental investigation of interfacial instability in separated blood. *AIChE J*. 2019;65(4):1376-1386.
33. Wintrobe MM. Macroscopic examination of the blood: discussion of its value and description of the use of a single instrument for the determination of sedimentation rate, volume of packed red cells, leukocytes and platelets, and of icterus index. *Am J Med Sci*. 1933;185(1):58-70.
34. Sajeesh P, Doble M, Sen AK. Hydrodynamic resistance and mobility of deformable objects in microfluidic channels. *Biomicrofluidics*. 2014; 8(5):054112.
35. Gross M, Kruger T, Varnik F. Rheology of dense suspensions of elastic capsules: normal stresses, yield stress, jamming and confinement effects. *Soft Matter*. 2014;10(24):4360-4372.

SUPPORTING INFORMATION

Additional supporting information may be found online in the Supporting Information section at the end of this article.

How to cite this article: Pitt WG, Alizadeh M, Blanco R, et al. Factors affecting sedimentational separation of bacteria from blood. *Biotechnol Progress*. 2019;e2829. <https://doi.org/10.1002/btpr.2892>